Marine Environmental Research 192 (2023) 106238

Contents lists available at ScienceDirect

Marine Environmental Research

journal homepage: www.elsevier.com/locate/marenvrev

The role epiphytes play in particle capture of seagrass canopies

Aina Barcelona [a,*], Jordi Colomer [a], Teresa Serra [a], Damboia Cossa [b,c], Eduardo Infantes [d]

[a] Department of Physics, University of Girona, 17071, Girona, Spain
[b] Department of Marine Sciences, Kristineberg, University of Gothenburg, 45178, Sweden
[c] Eduardo Mondlane University, Department of Biological Sciences, Maputo, Mozambique
[d] Department of Biological and Environmental Sciences, Kristineberg, University of Gothenburg, 45178, Sweden

ARTICLE INFO

Keywords:
Seagrass
Eelgrass
Epiphyte
Sedimentation
Leaves capture
Suspension
Leaf length
Epiphytic area

ABSTRACT

Seagrass epiphytic communities act as ecological indicators of the quality status of vegetated coastal environments. This study aims to determine the effect leaf epiphytes has on the sediment capture and distribution from outside sources. Thirteen laboratory experiments were conducted under a wave frequency of 0.5 Hz. Three epiphyte models were attached to a *Zostera marina* canopy of 100 plants/m^2 density. The sediment deposited to the seabed, captured by the epiphytic leaf surface, and remaining in suspension within the canopy were quantified. This study demonstrated that the amount of epiphytes impacts on the sediment stocks. *Zostera marina* canopies with high epiphytic areas and long effective leaf heights may increase the sediment captured on the epiphyte surfaces. Also, reducing suspended sediment and increasing the deposition to the seabed, therefore enhancing the clarity of the water column. For largest epiphytic areas, a 34.5% increase of captured sediment mass is observed. The sediment trapped on the leaves can be 10 times greater for canopies with the highest epiphytic areas than those without epiphytes. Therefore, both the effective leaf length and the level of epiphytic colonization are found to determine the seagrass canopy ability at distributing sediment.

1. Introduction

Coastal ecosystems are colonized by seagrass meadows that provide significant ecological and physical ecosystem services. For example, they act as refuge and nursery habitats for fish and macroinvertebrates (Unsworth et al., 2017), attenuate waves and turbulence (Gacia et al., 1999; Infantes et al., 2012; Pujol et al., 2013), reduce erosion with the roots (Infantes et al., 2022), stabilize the bottom through decreasing sediment resuspension (Ros et al., 2014) and enhance sediment trapping (Barcelona et al., 2021b, 2023a). Seagrass plants have a complex structure, with invertebrates and macroalgae growing on the leaves and rhizomes forming assemblages named epiphytes (Trautman and Borowitzka, 1999). The abundance of epiphytes depends on the available leaf area of the seagrass and can impact the growth of the seagrass itself by decreasing the light reaching the canopy and reducing water fluxes (Cambridge et al., 2007).

The presence of epiphytes on seagrass leaves suggests ecological indications and signals the quality status of vegetated coastal environments (Mutlu et al., 2022). Overall, the quantity and quality of epiphytes serve as indicators of the level of intensity and the spatial distribution of ecological and anthropogenic processes such as eutrophication, productivity, herbivory, acidification, seasonality, turbidity, pollution, sedimentation, hydrodynamics, among others (Baggett et al., 2010; Balata et al., 2008; Ben Brahim et al., 2020; Mutlu et al., 2022). Likewise, leaf growth is regulated to maintain a proportion of uncolonized leaf surface, and epiphyte coverage plays a role in its regulation. In *Zostera marina,* the rate of leaf emergence positively correlates with epiphyte load (Ruesink, 2016). Additionally, epiphyte biomass increases exponentially with leaf age during the first days of colonization, whereas for older leaves epiphytes do not change in biomass (Borum, 1987). Among the key processes, the patterns of the spatial variability of macro-epiphyte assemblages on *Posidonia oceanica* leaves differ in relation to anthropogenic interference in the Gulf of Gabes, with both biomass and mean percentage cover decreasing near a sewage outlet point compared to control locations (Ben Brahim et al., 2010). In *Cymodocea nodosa* and the invasive species *Halophila stipulucea*, shoot density and epiphytic biomass cover decreased when exposed to high levels of hydrodynamic activity (Ben Brahim et al., 2020). Seagrass epiphytes have been shown to progressively enrich seawater with minerals and nutrients (Brodersen and Kühl, 2022). However, high epiphytic colonization decreases light availability for seagrass leaves, thus increasing the diffusion distance between the leaf and the surrounding water, which

* Corresponding author.
E-mail address: aina.barcelona@udg.edu (A. Barcelona).

https://doi.org/10.1016/j.marenvres.2023.106238
Received 7 July 2023; Received in revised form 28 September 2023; Accepted 19 October 2023
Available online 21 October 2023

may result in basification, warming and/or hypoxia for the seagrass (Brodersen and Kühl, 2022).

Seagrass meadows are highly productive habitats that can act as "blue carbon sinks" in coastal ecosystems by facilitating sedimentation and trapping particles (Jankowska et al., 2016; Röhr et al., 2018). Most of the variation in carbon stocks has been explained by sediment mud content, dry carbon density and degree of sorting, salinity, and water depth, along with plant attributes such as biomass and shoot density (Röhr et al., 2018). Settling particles within an artificial seagrass canopy can be trapped by the plant leaves or settle to the bottom, increasing with the canopy coverage (Barcelona et al., 2023a) and decreasing with the wave frequency (Barcelona et al., 2021b). However, the amount of sediment trapped by each single plant leaf was lower for high canopy densities compared to low canopy densities. Both processes can act synergistically to reduce the exchange of light and gases that could harm seagrass canopy development. Moreover, the total amount of sediment trapped on the seagrass leaves increased linearly with patch length (Barcelona et al., 2023a), demonstrating the importance of canopy fragmentation in the trapping of sediment particles.

Epiphyte distribution on plant leaves can also modify the structure of the plants, impacting their flexural stiffness by modifying the cross-sectional area of the leaf (Fonseca and Koehl, 2006). In this case, the behaviour of a canopy can approach that of a rigid canopy and produce more turbulent kinetic energy or can approach a flexible canopy, i.e., moving with the flow and without producing turbulent kinetic energy (Barcelona et al., 2023b). Since hydrodynamics drive the capacity of seagrass to capture sediment particles (Barcelona et al., 2021b), it is worth determining how large amounts of sediment not only from coastal runoff, river plumes, natural resuspension, and heavy rains (Pineda et al., 2017; Vautard et al., 2014) but also from anthropogenic sources such as coastal development (Wu et al., 2018) reach seagrass meadows and are finally redistributed through the meadows. Therefore, it is expected that the distribution of epiphytes growing on plant leaves modifies sediment trapping capacity, thus regulating the sedimentation stocks in each canopy compartment. Indeed, suspended particles may be phagocyted by some seagrass epiphytes found on the leaves (Agawin and Duarte, 2002). Additionally, settling microplastics have been found to be trapped by seagrass (de los Santos et al., 2021), or adhere to eelgrass leaves and form biofilms, i.e., a sink of microplastics (Zhao et al., 2022).

The aim of the present study is to understand the role epiphytes on seagrass leaves have in the capture of sediment particles. The hypothesis of this study is formulated as follows: the area of the epiphytes colonizing a coastal canopy has the potential to modify the distribution and balance of sediment, including sediment suspended within the canopy, trapped by leaves and found on the canopy bed.

2. Methodology

2.1. Flume set-up

This study was conducted in the hydraulic flume at the Kristineberg Marine Research Station, Sweden (Fig. 1). The flume was 800 cm long, 50 cm wide, 50 cm deep and equipped with an electronic piston that generated waves at a frequency of f = 0.5 Hz. To prevent wave reflection at the end of the flume, a PVC beach with a 20° slope covered by synthetic fibre was placed at the end of the flume (Marin-Diaz et al., 2020; Serra et al., 2018). To simulate the natural conditions of the seagrass in the field, the flume was filled with seawater, directly from Gullmarn Fjord with a salinity of S = 27.65°/$_{oo}$ and the water temperature was T = 15 °C (± 1 °C). The mean water working height in the flume was h = 23 cm, and the test section was 200 cm long (Fig. 1), starting 300 cm from the wave generator. The bottom of the test section was filled with sandy sediment with a diameter of d_{50} = 0.8–2 mm. To minimise additional turbidity from the sandy sediment bottom, the flume was filled with water and immediately discarded to remove the resuspended small particle content from the bed. This process was carried out three times before starting the experiment. Finally, prior to each experiment run, the flume was filled with water and left under the action of the waves for 5 min.

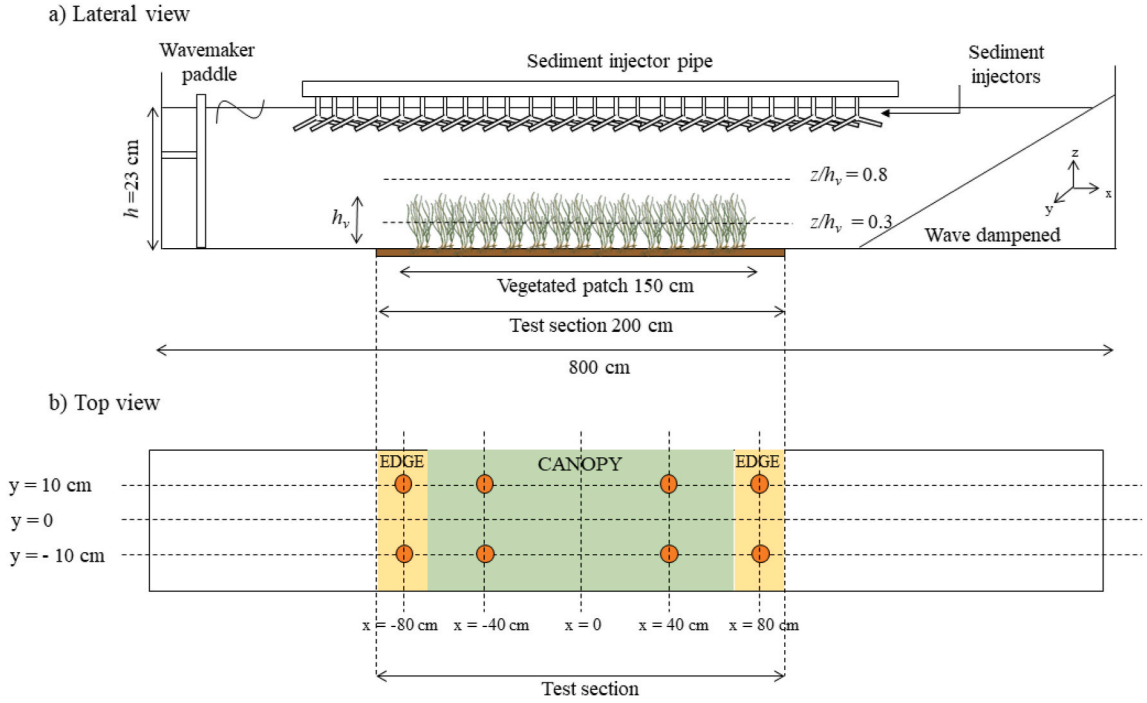

Fig. 1. Experimental setup and canopy regions with sediment trap locations, a) Lateral view of the experimental setup in the flume, with the wave paddle generator located on the left. Waves propagate from left to right. b) Top view of the setup illustrates two regions: the inner canopy region (in green) and the edge region of the canopy (in yellow). Additionally, orange circles indicate the position of sediment traps distributed along the flume bed in both the canopy and edge regions.

2.2. Vegetation

Eelgrass (*Zostera marina*) shoots were collected from the Gullmarn Fjord, located on the west coast of Sweden near the Kristineberg Marine Research Centre (58.25°N, 11.45° W). The seagrass meadows from the Gullmarn Fjord have been reported to be composed of *Z. marina* and *Zostera noltii* individuals, although, the eelgrass *Z. marina* is the most abundant one. Only *Z. marina* individuals were collected and used in the experiments. Since both *Zostera noltii* and *Z. marina* present the same morphology above ground, they are expected to behave similarly. Collection was carried out between June and August 2022 at a depth of 1–2 m. The eelgrass plants had an average of 3 ± 1 leaves·shoot^{-1}, with a shoot length of $h_p = 20 \pm 2$ cm, a shoot width of 0.4 ± 0.1 cm, and a thickness of 0.045 ± 0.005 cm. The plants were kept in laboratory tanks with flow-through seawater from the fjord. To prevent any scouring and uprooting of the plants in the flume, the rhizome and roots were separated, and each shoot was fixed to a wooden stick (3 cm long and 0.5 cm in diameter) with a cable tie. The stick and cable tie were then buried into the sediment. The vegetated area in the flume was 1.5 m long (Fig. 1a), with a plant density of $n = 100$ shoots·m^{-2} which falls within the range of shallow eelgrass densities found the west coast of Sweden (Boström et al., 2014).

2.3. Epiphyte distribution and treatments

To simulate the effect of the epiphyte cover, three macroalgae species, namely: *Fucus vesiculosus*, *Fucus serratus* and *Furcellaria lumbricalis* were used to represent three levels of epiphytic structure. *F. serratus* presents the simplest structure with laminar leaves, *F. vesiculosus* presents a greater complexity with laminar leaves but with aerocysts. In contrast, *F. lumbricalis* presents the most complex structure with a filamentous shape and with the greatest 3D morphology. These macroalgae species were chosen to represent various epiphyte morphology structures that can potentially be found attached to eelgrass leaves (García-Redondo et al., 2019). While these species may not commonly exist as epiphytes in eelgrass canopies, they were chosen due to their diverse morphologies which can be observed in actual epiphytes attached to eelgrass leaves. This selection allows for the simulation of different types of epiphytes that may occur naturally. Likewise, the constructed epiphyted covered the 35% of the plant leaf length according to the

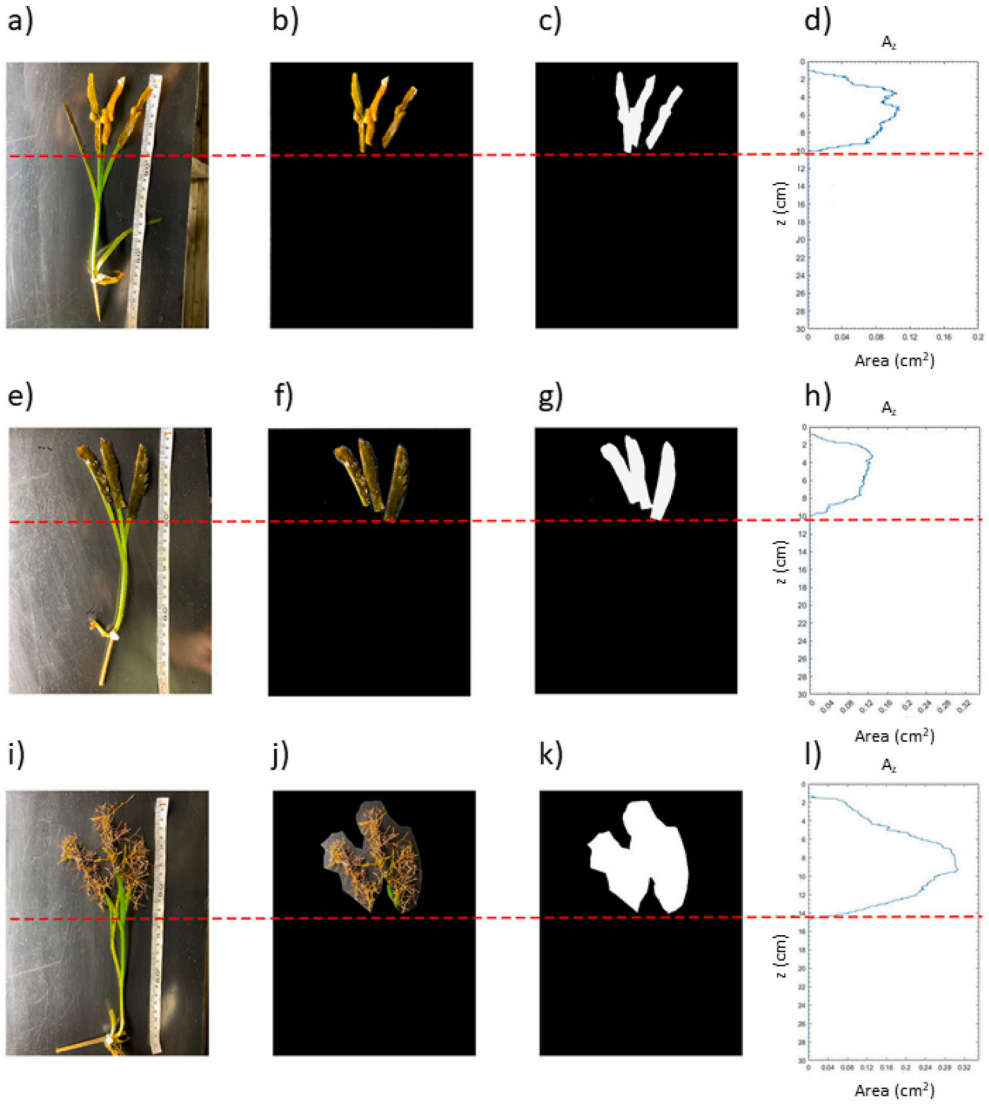

Fig. 2. Eelgrass shoots with epiphyted areas and vertical distribution of epiphyte coverage. Photograph of eelgrass shoots displaying the epiphytic area of a single plant located at the top of the leaves for the three epiphytes considered: *Fucus vesiculosus* (E1), *Fucus serratus* (E2, and *Furcellaria lumbricalis* (E3) (a, e, and i, respectively) (left panels). Furthermore, photographs of the epiphyte area for each type of species (central panels), and a plot illustrating the vertical distribution of the epiphyte area A_z with height for each type of epiphyte (d, h and l in the right panels) was generated.

percentages of epiphytes found in the field (Somma et al., 2023). This tries to mimic that in nature, epiphytes are more abundant in the apic part of the leaf than in the lower leaf sections (Reyes et al., 1998; Somma et al., 2023). The laboratory simulated epiphytic plants of epiphytic leaves with dimensions of 7 cm long x 0.5 cm wide piece of *F. serratus* or *F. vesiculosus* previously scraped with a scalpel to eliminate the epiphytic part on the algae, gently dried with a paper towel, and then glued to the eelgrass leaf with Loctite super glue. Therefore, each plant presented three epiphytic fragments; one for each leaf. In the case of *F. lumbricalis*, several 0.6 ± 0.1 cm fragments of *F. lumbricalis* were glued along the top 7-cm-long surface of the *Z. marina* leaves (Fig. 2). The simulated epiphytes covered the upper part of the leaves, which is considered the flexible portion of each plant (Barcelona et al., 2023b). From now on, the plants epiphyted with *F. vesiculosus, F. serratus* and *F. lumbricalis* will be referred to as E1, E2 and E3, respectively, because these algae species were used to model a natural epiphyte. Four epiphyted canopy distributions were used for each epiphyte type, E1, E2 and E3: 0 %, 25 %, 50 %, 75 % and 100% of the total number of plants of the canopy were epiphyted, resulting in 13 treatments (Table 1). Then, a total of 13 set ups were considered, one for each treatment.

The effective height of the eelgrass without epiphytes, which refers to the bending of leaves caused by the waves, was determined by calculating the mean of the maximum and minimum bending heights observed during 25 oscillations. This measurement was repeated three times. The effective heights measured for each epiphyted plant (E1, E2 and E3) were h_v = 16.00 ± 0.47, 17.13 ± 0.92, and 17.67 ± 1.05 respectively, and for the non-epiphyte plant experiment it was 17.96 ± 0.51 cm.

2.4. Sediment injection

The wavemaker was activated and allowed to operate for 15 min to establish equilibrium in the system before sediment injection. Synthetic dust powder (ISO 12103-1, A4 Coarse, Powder Technology Inc., Burnsville) was used as sediment in the experiment. The sediment A4 was composed by particles from 5 mm to 120 mm with a d50 = 41.7 μm (Barcelona et al., 2023a; Mancini et al., 2023). Therefore, it was composed from fine silts to fine sand particles. This is in accordance with the size of sediment particles composing river plumes (Grifoll et al., 2014).

The particle-laden flow for injection was prepared by taking an initial volume of sediment suspension (2 L), with a concentration of 120 g L^{-1}, which was then introduced into one end of the sediment-injector pipe. The injector pipe was positioned at y = 0 cm along the flume axis (Fig. 1a). During the sediment injection process, the injectors were oriented upwards to prevent any unintended spillage. Once the pipe was filled with the sediment suspension, it was closed and turned downward so that the injectors extended 5 cm below the water surface facing down. The injectors remained positioned at the top of the water column, above the vegetated patch, at a depth of 5 cm from the surface. Since the suspended sediment concentration in all the trials remained below 17.46 g L^{-1}, the sediment concentration was not expected to have any effect on the settling velocity of particles (Colomer et al., 1998).

The sediment injector pipe was a large 2.5 m-long pipe equipped with 42 sediment injectors evenly distributed 7 cm apart from each other. The design of the sediment injectors resembled a Y-shape, with a total length of 26 cm. Each arm of the injector pipe was 22.5 cm long (Fig. 1a). To ensure a uniform distribution of sediment, each arm of the pipe had 12 holes from which the sediment was released into the flume. This setup allowed for a homogeneous injection of sediment along both the x-axis and the y-axis of the flume.

Table 1
Summary of the conducted experiments.

Run	Epiphyted plants (%)	Epiphyte type
1	0%	non-epiphyted
2	25%	E1
3	50%	E1
4	75%	E1
5	100%	E1
6	25%	E2
7	50%	E2
8	75%	E2
9	100%	E2
10	25%	E3
11	50%	E3
12	75%	E3
13	100%	E3

2.5. Sediment measurements

To obtain the sediment concentration and distribution along the canopy, three types of sediment measurements were conducted: 1) sediment deposited on the bed, 2) suspended sediment, and 3) sediment attached to plant leaves with epiphytes.

Sediment deposition. To measure the sediment deposited on the bed, eight sediment traps were distributed in two rows along the main axis of the flume at y = ± 10 cm and x = 0 ± 40 cm, ±80 cm (Fig. 1b). Sediment samples from traps were collected at t = 60 min after the injection.

Suspended sediment. To measure suspended sediment, 50 mL water samples were pipetted at the same x position where the sediment traps were located for each run, at y = 0 cm, and at two water depths, at z/h_p = 0.3 (within the canopy) and at z/h_p = 0.8 (above the canopy). These sampling locations were chosen to provide representative measurements within and above the canopy. Water samples were collected at various time points (t = 2, 30 and 60 min) after the sediment injection, and were later analysed to determine the concentration levels of the suspended sediment.

Sediment trapping. To measure the influence of epiphytes on sediment trapping, five percentages of epiphyted seagrass leaves were considered in order to mimic natural occurrence observed in the field (Borowitzka et al., 2005). The following percentages of epiphyted leaves were examined: 0%, 25%, 50%, 75% and 100% of the plant leaves covered with epiphytes. For all the cases of 0% and 100%, three sets of five plants were collected for the analysis. For the cases of 25%, 50% and 75%, three sets of five epiphyted plants were collected, along with three sets of three epiphyted plants and two non-epiphyted for further analysis. In all cases, the plants were gently removed from the same x positions within the vegetated patch where the sediment traps had been placed at t = 60 min after the sediment injection. Afterwards, the plants were placed in a glass beaker with 100 mL of filtered seawater and stirred to remove the sediment trapped on the leaf surfaces or by the epiphytes.

To ensure the independency of the measurements a protocol was established. First, the suspended sediment samples were taken. Secondly, the sediment traps were covered with a lid. Thirdly, the fifteen plants were gently removed to measure the sediment trapped by the leaves and finally, the sediment traps were collected from the bottom of the flume and their content analysed.

The mass (in grams) of sediment in each sample was obtained by filtering them with glass microfiber filters (GF/F). The sediment traps and suspended sediment samples were filtered using filters with diameters of 50 mm and 25 mm, respectively. Firstly, the empty filters were weighted to obtain a zero weight. Then, the samples were filtered, dried at 60 °C over 24 h and then weighed again (Brouwer et al., 2023).

2.6. Measuring velocities

The Eulerian velocity field was defined as (u, v, w) in the (x, y, z) directions, respectively. The three components of the velocity were recorded with a downwards-facing Acoustic Doppler Velocimeter (ADV, Nortek, Vectrino) at a frequency of 25 Hz for 10 min, resulting in 15,000

measurements. Beam correlations less than 90% were discarded and spikes were removed (Goring and Nikora, 2002). The ADV was mounted on a movable vertical frame (at x = 0, Fig. 1b) and manually adjusted to measure at z = 5 cm, 6 cm, and 12 cm. Some plants were temporarily removed to prevent obstruction of the ADV beams (Zhang et al., 2018), and were re-inserted into the nearby area when measurements were completed.

For oscillatory flows, the instantaneous velocity, $U_i(t)$, can be decomposed as:

$$U_i(t) = U_c + Uw + u' \quad (1)$$

where, U_c is the mean current velocity associated to the wave, U_w is the unsteady wave motion which represents spatial variations in the phase-averaged velocity field, and u' is the turbulent velocity; that is, the instantaneous velocity fluctuation in the x-direction. U_c is the phase-averaged velocity:

$$U_c = \frac{1}{2\pi}\int_0^{2\pi} U_c(\varphi)\delta\varphi \quad (2)$$

where, $U_c(\varphi)$ is the instantaneous velocity according to the phase (Lowe et al., 2005; Luhar et al., 2010). In the current study, U_c at $z/h_v = 0.3$ above the bed (i.e., within the canopy layer) was always smaller than U_w, with mean values of -0.8 cm s^{-1}.

The wave velocity, U_w, was determined using a phase averaging technique. The Hilbert transform was used to average the oscillatory flow velocities with a common phase (Pujol et al., 2013; Ros et al., 2014). The root mean square (rms) of U_w was considered as the characteristic value of the orbital velocity U_w^{rms} (U_w hereafter) at each depth, and was calculated according to:

$$U_w^{rms} = \sqrt{\frac{1}{2\pi}\int_0^{2\pi} (U_i(\varphi) - Uc)^2\delta\varphi} \quad (3)$$

2.7. Theory

The sediment injected in the flume was distributed into four different compartments: captured by the epiphyted surface, deposited to the bottom, and remaining in suspension (above and within the canopy). A non-dimensional model was constructed based on the Pi-Buckingham theorem. Four variables and two dimensions were considered. The variables were the mass of sediment accumulated in each compartment (TM_i, where i = *b*, *s*, *p*, *ab*, where *b* represents sediment deposited at the bottom, *s* represents the sediment in suspension within the canopy, *p* represents the sediment deposited on the epiphyted surface of the plants and *ab* represents the sediment in suspension above the canopy), the sediment density (ρ), the total epiphyted area of the canopy (A) and the effective height (h_v). The dimensions were grams and metres. Therefore, two governing non-dimensional parameters can be constructed to describe the results. First, $TM_i/(A\rho h_v)$, representing the total mass of sediment captured by each compartment (TM_i) per total mass of the epiphyted canopy area, and second A/h_v^2, defined as the normalized area of the epiphyted meadow. This last parameter is a function of the normalized epiphyte length scale ($(L_{ep}/h_v)^2$), where L_{ep} is the epiphyte's length, which corresponded to the square root of A. A/h_v^2 indicates the increase in the frontal area between a non-epiphyted canopy and the different levels of epiphyted canopies. TM_p is the total mass of sediment collected by all plants in the canopy, obtained multiplying the mass of sediment collected by each single plant (M_p) by the number of plants in the canopy. TM_s is the total mass of sediment in suspension that was calculated by multiplying the mass of suspended sediment in the sample (M_s) by the ratio between the total volume within the canopy and the volume of the sample (100 mL). TM_b is the total mass of sediment deposited to the bottom that was calculated by multiplying the mass of sediment in the trap (M_b) by the ratio between the total area of the vegetated bottom and the area of a single trap (of 0.05×0.02 m^2).

Therefore, a non-dimensional model should consider the relationship between the above governing non-dimensional parameters. It is possible to expect:

$$\frac{TM_i}{A\rho hv} = f\left(\frac{A}{h_v^2}\right) = a\left(\frac{A}{h_v^2}\right)^c \quad (4)$$

where f is function of the dimensionless parameter A/h_v^2, and *a* and *c* are constants of the relationship.

The epiphyted area of each plant A_p was considered the effective area of the flow trapped inside the area of the epiphyte (Fig. 2). To obtain A_p, photographs of plants with epiphytes were converted to grayscale and later to black and white using MATLAB (MathWorks, Inc.). The threshold considered for the conversion to black and white corresponded to that representing the area of the region inside the epiphyte (Fig. 2a and b). The plant epiphyted area A_p was calculated as the vertical sum along the plant leaf of the area at each z (A_z) for each case (Fig. 2c). Therefore, the total epiphyted area of the canopy (A) was obtained multiplying A_p by the total number of epiphytes for each experiment.

2.8. Data analysis

TM_i was regressed against the percentage of epiphyted plant. The differences between the percentage of epiphyted plants and the epiphyted areas (A_p) were determined using ANOVA one-factor. The Shapiro-Wilk, and Levene's tests were performed to ensure normality and homogeneity.

3. Results

3.1. Distribution of sediment mass in the different compartments

The sediment was distributed into four compartments: sediment trapped by the seagrass leaves (Fig. 3a), sediment deposited on the bottom of the flume (Fig. 3b), sediment remaining in suspension within the canopy (Fig. 3c) and sediment remaining in suspension above the canopy (not considered). For the trials conducted with epiphytes E2 and E3, the mass of sediment, TM_p, trapped by all plant leaves increased linearly with the percentage of epiphyted plants (0%–100% epiphyted plants), following the tendencies for each epiphyte: $TM_p = 0.02$ (% epiphyted plants) + 0.75 for the E3 ($A_p = 94.51$ cm^2) and $TM_p = 0.01$ (% epiphyted plants) + 1.09 for the E2 ($A_p = 38.15$ cm^2) (Fig. 3a). However, for the lowest epiphyted area studied, corresponding to experiments with E1 ($A_p = 31.56$ cm^2), the mass of sediment trapped by plant leaves remained constant regardless of the percentage of epiphyted plants. In contrast, the mass of sediment deposited on the bottom did not show significant differences (p-value >0.05) between epiphyte types E1, E2 and E3, but did present a decreasing trend linearly correlated with the percentage of epiphyte plants, with a p-value <0.05 (Fig. 3b). In contrast, the sediment remaining in suspension did not show significant differences in relation to either the epiphyted area or the percentage of epiphyted plants (p-value >0.05, obtained by performing a one-way ANOVA) (Fig. 3c).

3.2. Non-dimensional model for sediment capture in each compartment

To quantify the sediment captured by the seagrass canopy, three non-dimensional models were developed to represent each compartment: sediment trapped by the plant leaves (Fig. 4), sediment deposited on the bottom (Fig. 5) and sediment remaining in suspension within the canopy (Fig. 6). These models were derived using Equation (4), as described in the Materials and Methods section.

For the sediment trapped by the plant leaves, a negative power trend

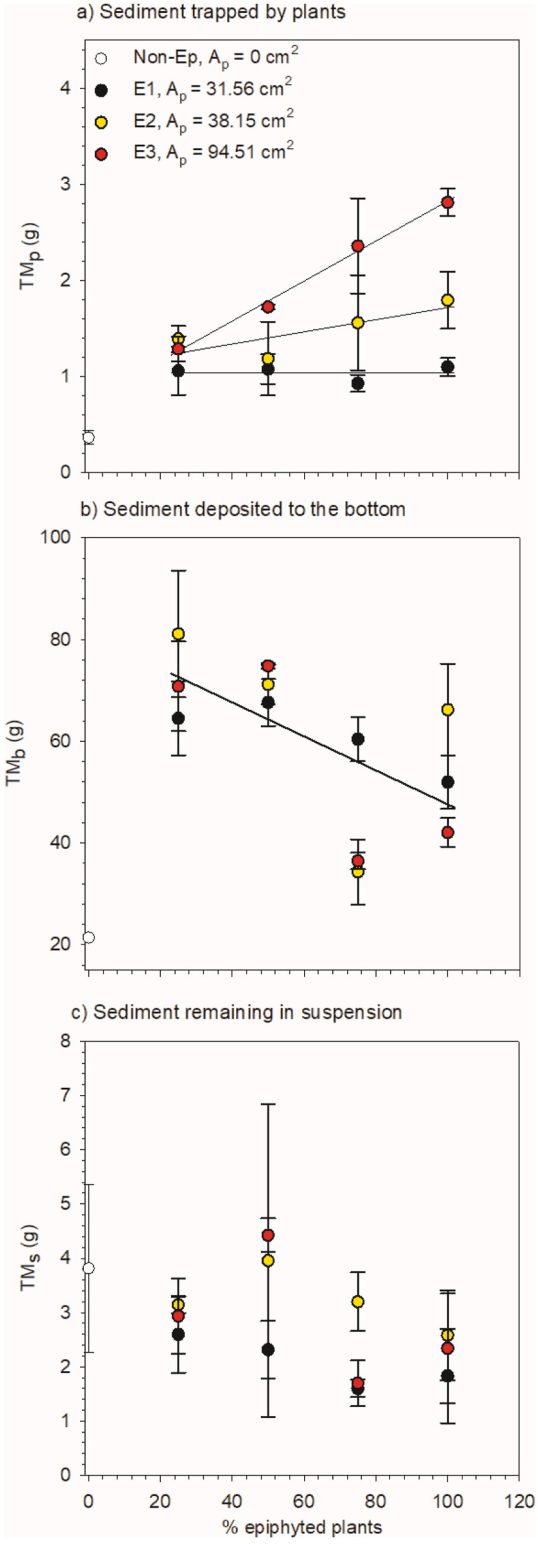

Fig. 3. Sediment distribution patterns associated with epiphyted plants. Mass of sediment a) trapped by plant leaves. The linear expressions for E2 and E3 found are: $TM_p = 0.02$ (% epiphyted plants) + 0.75 and $TM_p = 0.01$ (% epiphyted plants) + 1.09 respectively, p-value <0.05 in both cases, b) deposited to the bottom. The linear expression found is: $TM_b = -0.33$ (% epiphyted plants) + 81.00, p-value < 0.05 and c) remaining in suspension for the number epiphyted plants in the canopy (in percentage).

was found and is shown in Fig. 4. The expression has been solved for TM_p, following:

$$TM_p = 7{\cdot}10^{-5}\rho A^{0.27}h_v^{2.46}, \text{ with a } R^2 = 0.90 \quad [5]$$

and showing that the sediment trapped by the leaves increased with both the total epiphyted area A and the effective leaf length h_v (Fig. 4).

The non-dimensional mass deposited at the bottom in the complete area covered by vegetation, $TM_b/\rho Ah_v$, also presented a negative power trend with A/h_v^2 (Fig. 5). The dependence of the mass deposited at the bottom was obtained as a function of A and h_v, according to the following equation:

$$TM_b = 8.6{\cdot}10^{-3}\rho A^{-0.34}h_v^{3.68}, \text{ with a } R^2 = 0.94 \quad [6]$$

Therefore, the sediment deposited to the bottom depended negatively on the total epiphyted area (A) and positively on the effective height (h_v), as shown in Fig. 5. Equation (6) implies that the greater the epiphyted area, the lower the amount of sediment deposited to the bottom. However, the greater the effective height, the greater the amount of sediment deposited to the bottom (Fig. 5).

The sediment remaining in suspension within the total canopy region (TM_s), followed a negative power relationship (Fig. 6). The expression (as for the other compartments) was also solved by TM_s. TM_s decreased with the total epiphyted area (A) and increased with the effective height (h_v) with the following expression:

$$TM_s = 3{\cdot}10^{-4}\rho A^{-0.22}h_v^{3.43}, \text{ with a } R^2 = 0.92 \quad (7)$$

For the experiments conducted with 50% and 100% of epiphyted plants and for the different types of epiphytes, the total volume of sediment captured in each compartment (suspended, plant leaves, and bottom) was calculated. For the sediment trapped by the plant leaves, the total volume of sediment trapped was obtained as follows:

$$V_p = (M_{nep}\, N_{nep} + M_{ep}\, N_{ep}) / \rho \quad (8)$$

where N_{nep} and N_{ep} are the number of non-epiphyted and epiphyted plants, respectively. M_{nep} and M_{ep} are the mass of sediment captured by single both non-epiphyted and epiphyted plants, respectively.

For the sediment in suspension, the total volume of sediment within the canopy, V_s, was calculated as follows:

$$V_s = M_s\, L_p\, h_v / \rho \quad (9)$$

where L_p is the canopy length.

For the sediment deposited on the bottom, the total volume of sediment V_b was calculated as follows:

$$V_b = M_b\, L_p\, W \quad (10)$$

where W is the width of the flume.

The volume of particles deposited to the bottom (V_b) presented the largest percentage compared to the other two compartments (V_s and V_p). For the non-epiphytic case to the 100% of epiphyted plants (Fig. 7), the volume of sediment trapped by the plant leaves (V_p) increased with the total epiphyted area. The non-epiphytic case presented the lowest V_p = 0.6%, for the 50% of total epiphyted plants V_p increased from 1.5 to 2.1% with the total epiphyted area, and from 2.5 to 6.0% for the 100% of epiphyted plants (Fig. 7). In contrast, the volume of sediment deposited on the bottom (V_b) decreased with the total epiphyted area; being 93.5 for the non-epiphytic case, from 95% to 92.4% for the 50% epiphyted plants and from 93.8 to 90% for the 100% epiphyted plants (Fig. 7). V_s decreases with the presence of epiphytes, reaching a value of 5.9% for the non-epiphytic. However, V_s decreased as the total epiphytic area increased, from 3.3% to 5.1% for 50% of epiphyted plants and from 3.7% to 5.0% for experiments with 100% of epiphyted plants (Fig. 7).

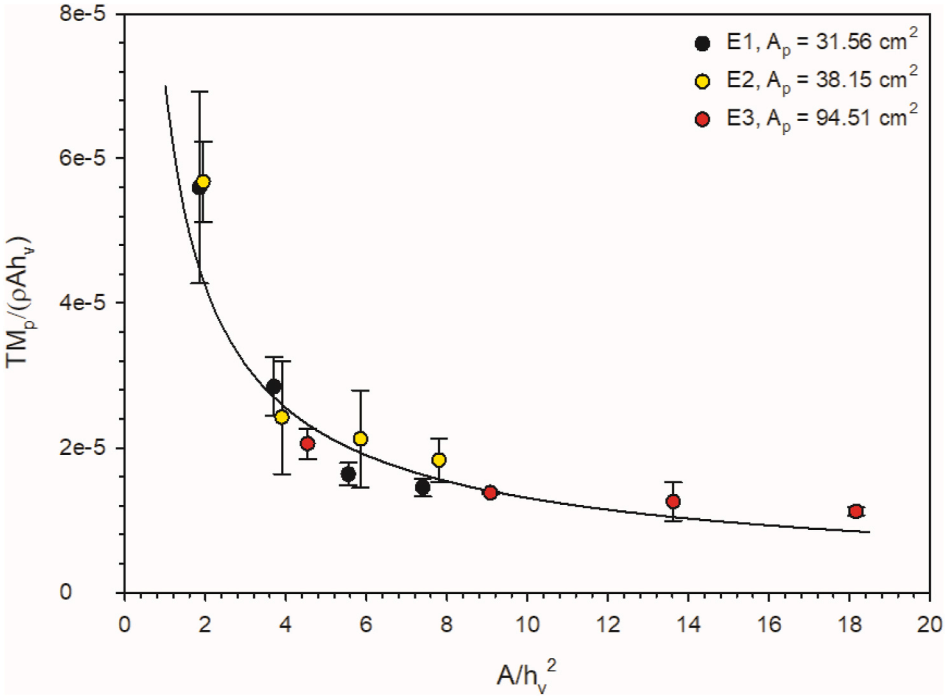

Fig. 4. Non-dimensional model for the mass sediment trapped by plant leaves, $TM_p/(\rho Ah_v)$ for the different A/h_v^2 tested. E1, A_p = 31.56 cm^2 (black filled circles), E2, A_p = 38.15 cm^2 (blue filled circles) and E3, A_p = 94.51 cm^2 (red filled circles). The power tendency found follows the expression: $TM_p/(\rho Ah_v) = 7{\cdot}10^{-5} (A/h_v^2)^{-0.73}$, with an $R^2 = 0.90$, p-value <0.05.

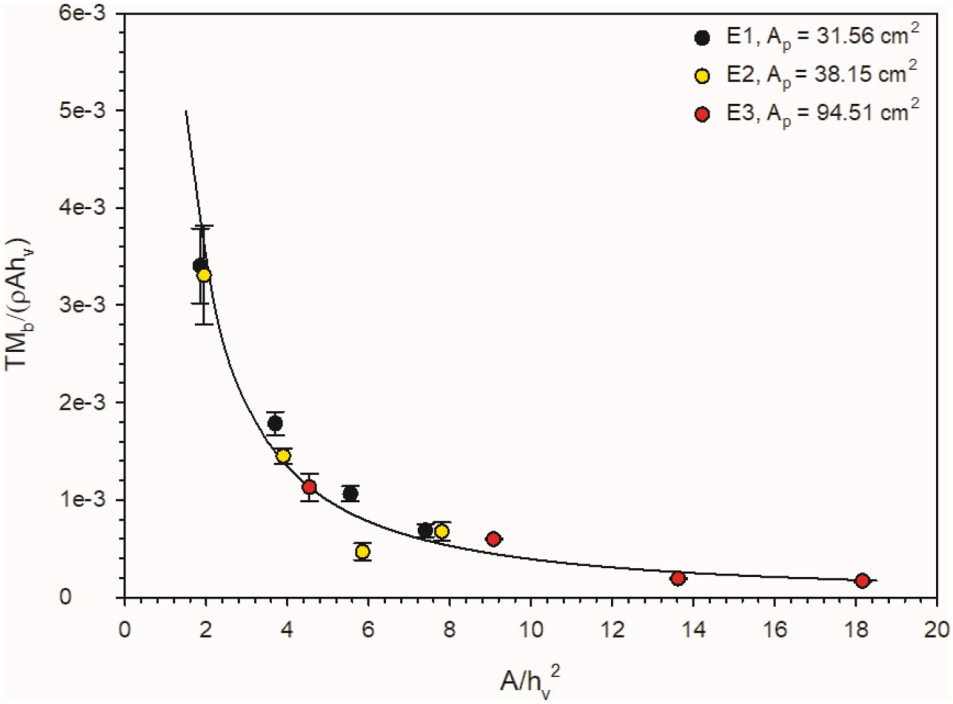

Fig. 5. Non-dimensional model for the mass sediment deposited to the bottom, $TM_b/(\rho Ah_v)$ for the different A/h_v^2 tested, E1, A_p = 31.56 cm^2 (black filled circles), E2, A_p = 38.15 cm^2 (blue filled circles) and E3, A_p = 94.51 cm^2 (red filled circles). The power tendency found follows the expression: $TM_p/(\rho Ah_v) = 8.6{\cdot}10^{-3} (A/h_v^2)^{-1.34}$, with an $R^2 = 0.94$, p-value <0.05.

4. Discussion

Seagrass habitats present a range of structural characteristics that affect the ecological services they provide (Ward et al., 2022). Factors such as plant stiffness, presence of bare sediment areas within seagrass canopies, leaf height, canopy density, stem diameter, patch length and presence of epiphytic communities, impact the functioning of seagrasses. This study demonstrates that sedimentation patterns at the bottom of epiphyted canopies and sediment capture by epiphyted leaves depend on both the effective height (h_v) of the plant and the total

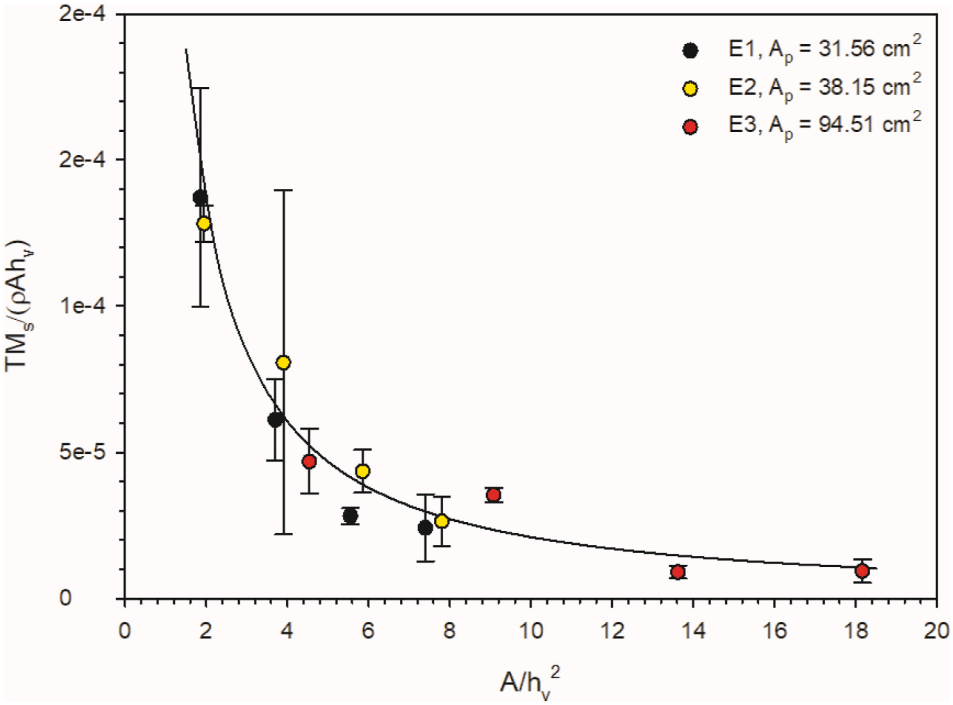

Fig. 6. Non-dimensional model for the mass sediment remained in suspension, $TM_s/(\rho Ah_v)$ for the different A/h_v^2 tested, E1, A_p = 31.56 cm^2 (black filled circles), E2, A_p = 38.15 cm^2 (blue filled circles) and E3, A_p = 94.51 cm^2 (red filled circles). The power tendency found follows the expression: $TM_s/(\rho Ah_v) = 3{\cdot}10^{-4}$ $(A/h_v^2)^{-1.22}$, with an R^2 = 0.92, p-value <0.05.

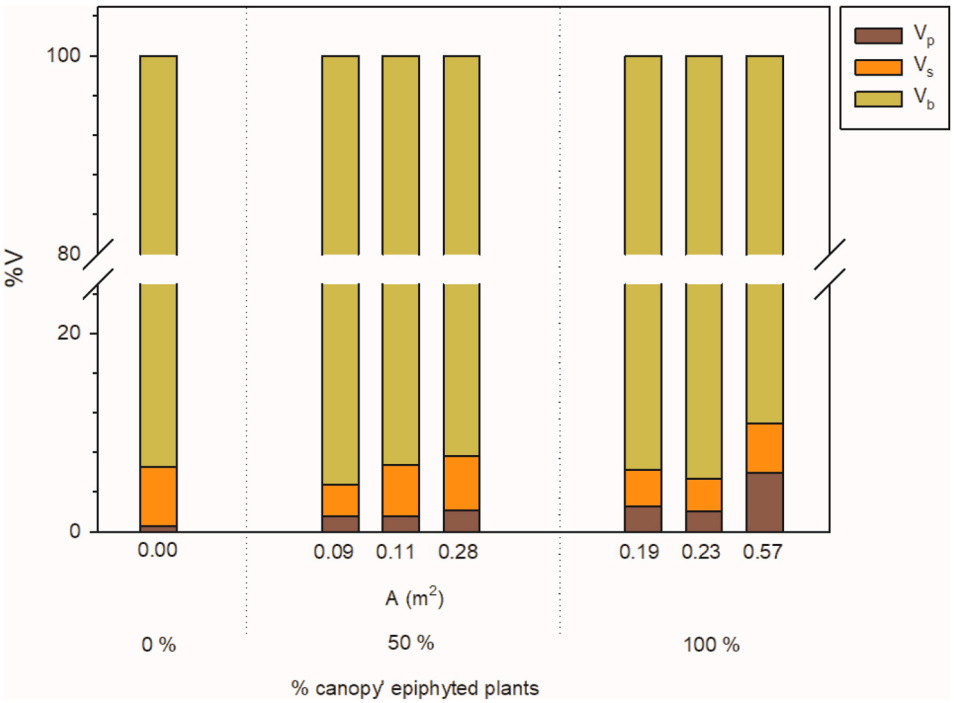

Fig. 7. Distribution of total sediment volume. Total sediment volume (V, in %) distributed in the different compartments: total volume of sediment trapped by the plant leaves (V_p), total volume of sediment, remaining in suspension within the canopy (V_s), and total volume of sediment deposited to the bottom (V_b) versus the total epiphytic area (A) for the cases 0%, 50% and 100% of epiphyted plants of the canopy. A (total epiphytic area), corresponds to each epiphyte used: E1 = 0.09; E2 = 0.11 and E3 = 0.28 m^2 for 50% of epiphyted plants and E1 = 0.19; E2 = 0.23 and E3 = 0.57 m^2 for 100% of epiphyted plants.

epiphyted area (A). Three types of epiphytic structures on eelgrass canopies were used to model three levels of epiphytic areas and compared to the non-epiphyted case.

The sediment trapped by the plant leaves was found to follow $TM_p = A^{0.27}h_v^{2.46}$. Therefore, the total mass of sediment attached to plant leaves increased with both the total epiphytic area and plant height. Increasing the effective plant height by 3.2% (when comparing E2 and E3) and 10.4% (when comparing E1 and E3) resulted in an increase in the total

mass of sediment captured on the plant leaves of 7.9%–27.7%, respectively. Similarly, increasing the total epiphytic area by 2.5 and 3 (comparing E2 and E3, and E1 and E3, respectively) led to an increase in the total mass of sediment attached to the leaves of 27.7% and 34.5%, respectively. As the accumulation of sediment on plant leaves increases with the epiphytic area, it might produce a negative feedback on seagrasses, reducing their gas exchange capabilities (Pujol et al., 2019) and their ability to meet light requirements (Brodersen and Kühl, 2022), due to the presence of epiphytes leading to a build-up on the diffusive boundary layer which may impeded oxygen transfer between the seagrass leaf and the surrounding water (Noisette et al., 2020). However, this negative effect might be counteracted in dense canopies, which capture less sediment per plant leaf but a higher overall amount when considering the sediment captured by the entire canopy (Barcelona et al., 2021b). Furthermore, the mass of sediment in suspension slightly decreases with the epiphytic area following $TM_s = A^{-0.33}h_v^{3.43}$. That is, the presence of epiphytes on the surface of the plant leaves reduces the mass of suspended sediment, resulting in a clearer water column. This result partially counteracts the negative effects of epiphyte presence, which otherwise would reduce the light availability and compromise the light requirements for plant leaves (Brodersen and Kühl, 2022).

The mass of sediment deposited at the bottom was found to depend on A and h_v following the relationship $TM_b = A^{-0.34}h_v^{3.68}$. This indicates that larger epiphytic areas increase the capture of sediment by plant leaves, resulting in a reduction of the sediment reaching the bottom. Additionally, the mass of sediment settling at the bottom increased with the effective plant height, indicating that higher plant leaves provide a greater surface area for particle capture (Borum, 1987; Ruesink, 2016). Stiffer plants, associated with higher effective plant heights, are expected to enhance the chances of particles settling to the bottom, increasing the overall sediment mass deposited in the bed.

In the absence of epiphytes, the majority of sediment particles, particularly those in the silt and clay ranges, reached the seagrass bottom (93.5%), while only a small portion was trapped by the plant leaves (0.6%). When the entire canopy was epiphyted (100% of plants in the canopy were epiphyted), the sedimentation at the seagrass bottom diminished to 90.0%, while the particles captured by the epiphyted leaves increased to 6.0%. Notably, the epiphyte with the greater surface area (E3), captured 10 times more sediment on the leaves when compared to the non-epiphyted canopy. In all cases with epiphytes, the volume of suspended sediment was lower than in cases without epiphytes. Therefore, colonization of epiphytes on eelgrass leaves may regulate the sedimentation stocks in each canopy compartment and reduce the amount of suspended sediment within the canopy, enhancing the role of the seagrass in clearing the water column.

However, in cases with a high epiphytic area, the presence of epiphytes on seagrass leaves, along with an increase in the sediment captured by leaves might lead to a reduction in available light, which is essential for plant requirements (Brodersen and Kühl, 2022). While moderate epiphytic cases may modulate light harvesting, high percentages of epiphytes can have a negative effect on seagrasses, compromising the survival of the canopy (Brodersen and Kühl, 2022). Generally, there is higher leaf growth and productivity at the centre of a seagrass meadow than at the edges (Turner, 2007). However, in dense seagrass beds, light competition can result in greater productivity at the edges compared to the centre (Nakaoka and Aioi, 1999). Also, a high epiphytic community growing on long seagrass leaves in the centre of a meadow might also compromise the seagrass, which experiences less light stress at the edges compared to the centre.

The percentage of epiphytic area was found to have no effect on eelgrass growth up to 60% (Ruesink, 2016). However, other studies have found a reduction in seagrass productivity with an increase in epiphyte mass (Reynolds et al., 2014; Whalen et al., 2013). Therefore, differences in seagrass responses to epiphytic areas might arise when resources are below saturating levels (Sand-Jensen, 1977), which could explain variations found between studies.

The variation in canopy epiphytic area may also impact the flexural capacity of plants, resulting in more rigid or more flexible structures which can modify plant behaviour under different hydrodynamic conditions. Rigid plants can produce more turbulent kinetic energy than flexible plants can (Barcelona et al., 2023b), which subsequently reduces the thickness of the diffuse boundary layer through increased flow velocity (Pujol et al., 2019) and potentially alters nutrient uptake (Cornelisen and Thomas, 2004).

Eelgrass, being an annual species, undergoes variations in leaf length during the year (Olesen and Sand-Jensen, 1994), resulting in seasonal changes in the available leaf area for epiphytes (Brodersen and Kühl, 2022). The non-dimensional model proposed indicates that the ecological function of the seagrass leaves in capturing sediment is going to vary following an annual cycle. Therefore, these seasonal variations in epiphytes may play a significant role in the sediment retention in coastal areas. This ecological service provided by eelgrass is of relevance considering the observed increase in heavy rainfall events that produce particle sediment-laden plumes in Europe in recent years (Vautard et al., 2014). Epiphytes also contribute to reducing the impact of the sediment output from the dredging activities related to coastal development (Wu et al., 2018).

Therefore, the structural characteristics of plant and canopies, in addition to hydrodynamic conditions, time of the year, and imposed natural or anthropogenic disturbances, are crucial factors for the development of seagrass habitats (Barcelona et al., 2021a, 2021b, 2021c, 2023a, 2023b; Duarte et al., 2005, 2013; Eckardt et al., 2023; Granata et al., 2001; Hendriks et al., 2008). As shown in this study, epiphyte presence on plant leaves is also a key component to consider when determining the overall behavior of the canopy and its role in the capture of sediment from sediment output sources.

The hypothesis raised in the introduction has been confirmed. That is, the morphology and quantity of the epiphytes colonizing a *Z. marina* meadow have been found to be enhance the capture of particles by seagrass leaves, with epiphytes possessing larger effective areas capable of trapping more particles compared to those with smaller epiphytic areas. This behavior impacts on the other compartments. Then, the epiphytic community has been also found to modify both the deposition of sediment on the bed and the suspended sediment, with a decrease of the sediment deposited and the sediment suspended as the epiphytic area increased. These laboratory results a first step to understand the role of real epiphytic communities in the field in trapping suspended particles.

5. Conclusions

The current study demonstrates the significant role epiphytes play in the capture of sediment by an eelgrass canopy under an oscillatory flow regime. Three epiphyte models were used to quantify the impact their morphology has on sediment capture. Sediment particles originating from an external source interacted with the canopy, either becoming trapped on the epiphytic surfaces of plant leaves, remaining suspended within the canopy, or settling to the bottom bed. The mass of sediment trapped by the epiphytic leaves, accumulated within the canopy bed, and remaining in suspension, was found to be a function of the effective plant height (h_v) and the total epiphytic area (A).

This study demonstrates that eelgrass canopies with higher epiphytic leaf areas and longer effective leaf lengths (h_v) are prone to increase the mass sediment captured by the epiphyted plants. Longer plant leaves are expected to provide a greater surface area for epiphyte attachment compared to shorter leaves. Therefore, canopies with higher epiphyted cover would promote an increase in the sediment capture by plants, thereby reducing the amount of sediment that reaches the seabed. The magnitude of sediment mass trapped by the epiphyted canopy is particularly pronounced for canopies with the largest epiphytic areas, with a 34.5% increase compared to canopies with smaller epiphytic areas. For the epiphyte with the greatest surface area, the sediment mass

trapped within the leaves can be 10 times greater than that captured by leaves without epiphytes.

This study also demonstrates eelgrass meadow vulnerability when subjected to extensive epiphytic growth, as it leads to a substantial accumulation of sediment on seagrass leaves, which can pose challenges to plant survival by reducing gas exchange and light availability. Therefore, the fate of a meadow might be dependent on the balance between the different structural parameters including the canopy density and extension, and effective leaf length, and epiphytic area. This manuscript has shown the effect of the effective leaf length and the epiphytic area that, collectively, may modify the overall functioning of an eelgrass meadow.

CRediT authorship contribution statement

Aina Barcelona: Conceptualization, Data curation, Formal analysis, Methodology, Writing-original draft, Writing-review & editing. Jordi Colomer: Data curation, Writing-review & editing. Teresa Serra: Writing-review & editing, Funding acquisition. Damboia Cossa: Writing-review & editing. Eduardo Infantes: Conceptualization, Writing-review & editing, Funding acquisition, Supervision.

Declaration of competing interest

The authors declare that they have no known competing financial interests or personal relationships that could have appeared to influence the work reported in this paper.

Data availability

Data will be made available on request.

Acknowledgements

We would like to thank FORMAS grant Dnr. 2019-01192. We would also like to thank Michael Gitzen, Tristan Dickinson, and Kirsten Wohak for the field and laboratory assistance. This work was supported by the Ministerio de Economía y Competitividad of the Spanish Government through Grant PID2021-123860OB-100. Aina Barcelona was funded by the pre-doctoral grant 2020 FI SDUR 00043 from the “Generalitat de Catalunya”.

References

Agawin, N.S.R., Duarte, C.M., 2002. Evidence of direct particle trapping by a tropical seagrass meadow. Estuaries 25, 1205–1209. https://doi.org/10.1007/BF02692217.

Baggett, L.P., Heck, K.L.J., Frankovich, T.A., Armitage, A.R., Fourqurean, J.W., 2010. Nutrient enrichment, grazer identity, and their effects on epiphytic algal assemblages: field experiments in subtropical turtlegrass Thalassia testudinum meadows. Mar. Ecol. Prog. Ser. 406, 33–45. https://doi.org/10.3354/meps08533.

Balata, D., Bertocci, I., Piazzi, L., Nesti, U., 2008. Comparison between epiphyte assemblages of leaves and rhizomes of the seagrass Posidonia oceanica subjected to different levels of anthropogenic eutrophication. Estuar. Coast Shelf Sci. 79, 533–540. https://doi.org/10.1016/j.ecss.2008.05.009.

Barcelona, A., Colomer, J., Serra, T., 2023a. Spatial sedimentation and plant captured sediment within seagrass patches. Mar. Environ. Res. 188, 105997 https://doi.org/10.1016/j.marenvres.2023.105997.

Barcelona, A., Colomer, J., Serra, T., 2023b. Stem stiffness functionality in a submerged canopy patch under oscillatory flow. Sci. Rep. 13, 1904. https://doi.org/10.1038/s41598-023-28077-2.

Barcelona, A., Colomer, J., Soler, M., Gracias, N., Serra, T., 2021a. Meadow fragmentation influences Posidonia oceanica density at the edge of nearby gaps. Estuar. Coast Shelf Sci. 249, 107106 https://doi.org/10.1016/j.ecss.2020.107106.

Barcelona, A., Oldham, C., Colomer, J., Garcia-Orellana, J., Serra, T., 2021b. Particle capture by seagrass canopies under an oscillatory flow. Coast. Eng. 169, 103972 https://doi.org/10.1016/j.coastaleng.2021.103972.

Barcelona, A., Oldham, C., Colomer, J., Serra, T., 2021c. Functional dynamics of vegetated model patches: the minimum patch size effect for canopy restoration. Sci. Total Environ. 795, 148854 https://doi.org/10.1016/j.scitotenv.2021.148854.

Ben Brahim, M., Hamza, A., Hannachi, I., Rebai, A., Jarboui, O., Bouain, A., Aleya, L., 2010. Variability in the structure of epiphytic assemblages of Posidonia oceanica in relation to human interferences in the Gulf of Gabes, Tunisia. Mar. Environ. Res. 70, 411–421. https://doi.org/10.1016/j.marenvres.2010.08.005.

Ben Brahim, M., Mabrouk, L., Hamza, A., Jribi, I., 2020. Comparison of spatial scale variability of shoot density and epiphytic leaf assemblages of Halophila stipulacea and Cymodocea nodosa on the Eastern Coast of Tunisia. Plant Biosystems - An International Journal Dealing with all Aspects of Plant Biology 154, 413–426. https://doi.org/10.1080/11263504.2019.1674399.

Borowitzka, M.A., Lavery, P.S., van Keulen, M., 2005. Epiphytes of seagrasses. In: Seagrass:Biology, Ecologyl and Conservation. Springer Netherlands, Dordrecht, pp. 441–461. https://doi.org/10.1007/978-1-4020-2983-7_19.

Borum, J., 1987. Dynamics of epiphyton on eelgrass (Zostera marina L.) leaves: relative roles of algal growth, herbivory, and substratum turnover. Limnol. Oceanogr. 32, 986–992. https://doi.org/10.4319/lo.1987.32.4.0986.

Boström, C., Baden, S., Bockelmann, A., Dromph, K., Fredriksen, S., Gustafsson, C., Krause-Jensen, D., Möller, T., Nielsen, S.L., Olesen, B., Olsen, J., Pihl, L., Rinde, E., 2014. Distribution, structure and function of Nordic eelgrass *(Zostera marina)* ecosystems: implications for coastal management and conservation. Aquat. Conserv. 24, 410–434. https://doi.org/10.1002/aqc.2424.

Brodersen, K.E., Kühl, M., 2022. Effects of epiphytes on the seagrass phyllosphere. Front. Mar. Sci. 9 https://doi.org/10.3389/fmars.2022.821614.

Brouwer, S., Humphries, P., Holland, A., McCasker, N., 2023. Effect of suspended sediment concentration on the clearance and biodeposition rates of an Australian freshwater mussel (Hyriidae: Alathyria jacksoni). Freshw. Biol. https://doi.org/10.1111/fwb.14137.

Cambridge, M., How, J., Lavery, P., Vanderklift, M., 2007. Retrospective analysis of epiphyte assemblages in relation to seagrass loss in a eutrophic coastal embayment. Mar. Ecol. Prog. Ser. 346, 97–107. https://doi.org/10.3354/meps06993.

Colomer, J., Ross, J.A., Casamitjana, X., 1998. Sediment entrainment in karst basins. Aquat. Sci. 60, 338. https://doi.org/10.1007/s000270050045.

Cornelisen, C.D., Thomas, F.I.M., 2004. Ammonium and nitrate uptake by leaves of the seagrass Thalassia testudinum: impact of hydrodynamic regime and epiphyte cover on uptake rates. J. Mar. Syst. 49, 177–194. https://doi.org/10.1016/j.jmarsys.2003.05.008.

de los Santos, C.B., Krång, A.-S., Infantes, E., 2021. Microplastic retention by marine vegetated canopies: simulations with seagrass meadows in a hydraulic flume. Environ. Pollut. 269, 116050 https://doi.org/10.1016/j.envpol.2020.116050.

Duarte, C.M., Losada, I.J., Hendriks, I.E., Mazarrasa, I., Marbà, N., 2013. The role of coastal plant communities for climate change mitigation and adaptation. Nat. Clim. Change 3, 961–968. https://doi.org/10.1038/nclimate1970.

Duarte, C.M., Middelburg, J.J., Caraco, N., 2005. Major role of marine vegetation on the oceanic carbon cycle. Biogeosciences 2, 1–8. https://doi.org/10.5194/bg-2-1-2005.

Eckardt, N.A., Ainsworth, E.A., Bahuguna, R.N., Broadley, M.R., Busch, W., Carpita, N.C., Castrillo, G., Chory, J., DeHaan, L.R., Duarte, C.M., Henry, A., Jagadish, S.V.K., Langdale, J.A., Leakey, A.D.B., Liao, J.C., Lu, K.-J., McCann, M.C., McKay, J.K., Odeny, D.A., Jorge de Oliveira, E., Platten, J.D., Rabbi, I., Rim, E.Y., Ronald, P.C., Salt, D.E., Shigenaga, A.M., Wang, E., Wolfe, M., Zhang, X., 2023. Climate change challenges, plant science solutions. Plant Cell 35, 24–66. https://doi.org/10.1093/plcell/koac303.

Fonseca, M.S., Koehl, M.A.R., 2006. Flow in seagrass canopies: the influence of patch width. Estuar. Coast Shelf Sci. 67, 1–9. https://doi.org/10.1016/j.ecss.2005.09.018.

Gacia, E., Granata, T.C., Duarte, C.M., 1999. An approach to measurement of particle flux and sediment retention within seagrass (Posidonia oceanica) meadows. Aquat. Bot. https://doi.org/10.1016/S0304-3770(99)00044-3.

García-Redondo, V., Bárbara, I., Díaz-Tapia, P., 2019. Biodiversity of epiphytic macroalgae (Chlorophyta, Ochrophyta and Rhodophyta) on leaves of Zostera marina in the northwestern Iberian Peninsula. An. del Jardín Botánico Madr. 76, 78. https://doi.org/10.3989/ajbm.2502.

Goring, D.G., Nikora, V.I., 2002. Despiking Acoustic Doppler velocimeter Data. J. Hydraul. Eng. 128, 117–126. https://doi.org/10.1061/(ASCE)0733-9429(2002)128:1(117).

Granata, T.C., Serra, T., Colomer, J., Casamitjana, X., Duarte, C., Gacia, E., 2001. Flow and particle distributions in a nearshore seagrass meadow before and after a storm. Mar. Ecol. Prog. Ser. 218, 95–106. https://doi.org/10.3354/meps218095.

Grifoll, M., Gracia, V., Aretxabaleta, A., Guillén, J., Espino, M., Warner, J., 2014. Formation of fine sediment deposition from a flash flood river in the Mediterranean Sea. J. Geophys. Res-Oceans. 119 (9), 5837–5853. https://doi.org/10.1002/2014JC010187.

Hendriks, I.E., Sintes, T., Bouma, T.J., Duarte, C.M., 2008. Experimental assessment and modeling evaluation of the effects of the seagrass Posidonia oceanica on flow and particle trapping. Mar. Ecol. Prog. Ser. 356, 163–173. https://doi.org/10.3354/meps07316.

Infantes, E., Hoeks, S., Adams, M., van der Heide, T., van Katwijk, M., Bouma, T., 2022. Seagrass roots strongly reduce cliff erosion rates in sandy sediments. Mar. Ecol. Prog. Ser. 700, 1–12. https://doi.org/10.3354/meps14196.

Infantes, E., Orfila, A., Simarro, G., Terrados, J., Luhar, M., Nepf, H., 2012. Effect of a seagrass (Posidonia oceanica) meadow on wave propagation. Mar. Ecol. Prog. Ser. 456, 63–72. https://doi.org/10.3354/meps09754.

Jankowska, E., Michel, L.N., Zaborska, A., Włodarska-Kowalczuk, M., 2016. Sediment carbon sink in low-density temperate eelgrass meadows (Baltic Sea). J Geophys Res Biogeosci 121, 2918–2934. https://doi.org/10.1002/2016JG003424.

Lowe, R.J., Koseff, J.R., Monismith, S.G., Falter, J.L., 2005. Oscillatory flow through submerged canopies: 2. Canopy mass transfer. J. Geophys. Res. 110, C10017 https://doi.org/10.1029/2004JC002789.

Luhar, M., Coutu, S., Infantes, E., Fox, S., Nepf, H., 2010. Wave-induced velocities inside a model seagrass bed. J Geophys Res Oceans 115. https://doi.org/10.1029/2010JC006345.

Mancini, M., Serra, T., Colomer, J., Solari, L., 2023. Suspended sediments mediate microplastic sedimentation in unidirectional flows. Sci. Total Environ. 890 https://doi.org/10.1016/j.scitotenv.2023.164363.

Marin-Diaz, B., Bouma, T.J., Infantes, E., 2020. Role of eelgrass on bed-load transport and sediment resuspension under oscillatory flow. Limnol. Oceanogr. 65, 426–436. https://doi.org/10.1002/lno.11312.

Mutlu, E., Karaca, D., Duman, G.S., Şahin, A., Özvarol, Y., Olguner, C., 2022. Seasonality and phenology of an epiphytic calcareous red alga, Hydrolithon boreale, on the leaves of Posidonia oceanica (L) Delile in the Turkish water. Environ. Sci. Pollut. Control Ser. 30, 17193–17213. https://doi.org/10.1007/s11356-022-23333-w.

Nakaoka, M., Aioi, K., 1999. Growth of seagrass Halophila ovalis at dugong trails compared to existing within-patch variation in a Thailand intertidal flat. Mar. Ecol. Prog. Ser. 184, 97–103. https://doi.org/10.3354/meps184097.

Noisette, F., Depetris, A., Kühl, M., Brodersen, K.E., 2020. Flow and epiphyte growth effects on the thermal, optical and chemical microenvironment in the leaf phyllosphere of seagrass (Zostera marina). J. R. Soc. Interface 17, 20200485. https://doi.org/10.1098/rsif.2020.0485.

Olesen, B., Sand-Jensen, K., 1994. Demography of shallow eelgrass (Zostera marina) Populations–shoot dynamics and biomass development. J. Ecol. 82, 379. https://doi.org/10.2307/2261305.

Pineda, M.-C., Strehlow, B., Kamp, J., Duckworth, A., Jones, R., Webster, N.S., 2017. Effects of combined dredging-related stressors on sponges: a laboratory approach using realistic scenarios. Sci. Rep. 7, 5155. https://doi.org/10.1038/s41598-017-05251-x.

Pujol, D., Abdolahpour, M., Lavery, P.S., McMahon, K., Oldham, C., 2019. Flow velocity and nutrient uptake in marine canopies. Mar. Ecol. Prog. Ser. 622, 17–30. https://doi.org/10.3354/meps12987.

Pujol, D., Serra, T., Colomer, J., Casamitjana, X., 2013. Flow structure in canopy models dominated by progressive waves. J. Hydrol. (Amst.) 486, 281–292. https://doi.org/10.1016/j.jhydrol.2013.01.024.

Reyes, J., Sanson, M., Afonso-Carrillo, J., 1998. Distribution of the Epiphytes along the Leaves of Cymodocea Nodosa in the Canary Islands. Botanica Marina.

Reynolds, P.L., Richardson, J.P., Duffy, J.E., 2014. Field experimental evidence that grazers mediate transition between microalgal and seagrass dominance. Limnol. Oceanogr. 59, 1053–1064. https://doi.org/10.4319/lo.2014.59.3.1053.

Röhr, M.E., Holmer, M., Baum, J.K., Björk, M., Boyer, K., Chin, D., Chalifour, L., Cimon, S., Cusson, M., Dahl, M., Deyanova, D., Duffy, J.E., Eklöf, J.S., Geyer, J.K., Griffin, J.N., Gullström, M., Hereu, C.M., Hori, M., Hovel, K.A., Hughes, A.R., Jorgensen, P., Kiriakopolos, S., Moksnes, P.-O., Nakaoka, M., O'Connor, M.I., Peterson, B., Reiss, K., Reynolds, P.L., Rossi, F., Ruesink, J., Santos, R., Stachowicz, J. J., Tomas, F., Lee, K.-S., Unsworth, R.K.F., Boström, C., 2018. Blue carbon storage capacity of temperate eelgrass (Zostera marina) meadows. Global Biogeochem. Cycles 32, 1457–1475. https://doi.org/10.1029/2018GB005941.

Ros, À., Colomer, J., Serra, T., Pujol, D., Soler, M., Casamitjana, X., 2014. Experimental observations on sediment resuspension within submerged model canopies under oscillatory flow. Continent. Shelf Res. 91, 220–231. https://doi.org/10.1016/j.csr.2014.10.004.

Ruesink, J.L., 2016. Epiphyte load and seagrass performance are decoupled in an estuary with low eutrophication risk. J. Exp. Mar. Biol. Ecol. 481, 1–8. https://doi.org/10.1016/j.jembe.2016.03.022.

Sand-Jensen, K., 1977. Effect of epiphytes on eelgrass photosynthesis. Aquat. Bot. 3, 55–63. https://doi.org/10.1016/0304-3770(77)90004-3.

Serra, T., Oldham, C., Colomer, J., 2018. Local hydrodynamics at edges of marine canopies under oscillatory flows. PLoS One 13. https://doi.org/10.1371/journal.pone.0201737.

Somma, E., Terlizzi, A., Costantini, M., Madeira, M., Zupo, V., 2023. Global changes alter the successions of early Colonizers of benthic surfaces. J. Mar. Sci. Eng. 11, 1232. https://doi.org/10.3390/jmse11061232.

Trautman, D., Borowitzka, M., 1999. Distribution of the epiphytic organisms on Posidonia australis and P. sinuosa, two seagrasses with differing leaf morphology. Mar. Ecol. Prog. Ser. 179, 215–229. https://doi.org/10.3354/meps179215.

Turner, S.J., 2007. Growth and productivity of intertidal Zostera capricorni in New Zealand estuaries. N. Z. J. Mar. Freshw. Res. 41, 77–90. https://doi.org/10.1080/00288330709509897.

Unsworth, R.K.F., Williams, B., Jones, B.L., Cullen-Unsworth, L.C., 2017. Rocking the boat: damage to eelgrass by swinging boat moorings. Front. Plant Sci. 8 https://doi.org/10.3389/fpls.2017.01309.

Vautard, R., Gobiet, A., Sobolowski, S., Kjellström, E., Stegehuis, A., Watkiss, P., Mendlik, T., Landgren, O., Nikulin, G., Teichmann, C., Jacob, D., 2014. The European climate under a 2 °C global warming. Environ. Res. Lett. 9, 034006 https://doi.org/10.1088/1748-9326/9/3/034006.

Ward, E.A., Aldis, C., Wade, T., Miliou, A., Tsimpidis, T., Cameron, T.C., 2022. Is all seagrass habitat equal? Seasonal, spatial, and Interspecific variation in productivity dynamics within mediterranean seagrass habitat. Front. Mar. Sci. 9 https://doi.org/10.3389/fmars.2022.891467.

Whalen, M.A., Duffy, J.E., Grace, J.B., 2013. Temporal shifts in top-down vs. bottom-up control of epiphytic algae in a seagrass ecosystem. Ecology 94, 510–520. https://doi.org/10.1890/12-0156.1.

Wu, P.P.-Y., McMahon, K., Rasheed, M.A., Kendrick, G.A., York, P.H., Chartrand, K., Caley, M.J., Mengersen, K., 2018. Managing seagrass resilience under cumulative dredging affecting light: Predicting risk using dynamic Bayesian networks. J. Appl. Ecol. 55, 1339–1350. https://doi.org/10.1111/1365-2664.13037.

Zhang, Y., Tang, C., Nepf, H., 2018. Turbulent kinetic energy in submerged model canopies under oscillatory flow. Water Resour. Res. 54, 1734–1750. https://doi.org/10.1002/2017WR021732.

Zhao, L., Ru, S., He, J., Zhang, Z., Song, X., Wang, D., Li, X., Wang, J., 2022. Eelgrass (Zostera marina) and its epiphytic bacteria facilitate the sinking of microplastics in the seawater. Environ. Pollut. 292, 118337 https://doi.org/10.1016/j.envpol.2021.118337.